

MOELING AND PERFORMANCE ANALYSIS OF P-V SYSTEM BASED ON BRUSHLESS DC MOTOR

Sameh I. Selem, Hany M. Deeb, Mohamed A. Enany

Electrical Power and Machines Department, Faculty of Engineering, Zagazig University,

Zagazig, Egypt. 44519

Abstract: Recent studies on photo voltaic system (PVs) have concentrated on minimize the costs and maximize the conversion effectiveness. In order to maximize the effectiveness of PV energy conversion systems, solar panels should be operated at maximum power points (MPP). At MPP, solar arrays generate the electric energy at maximum efficiency and minimum losses. Solar cells have variable current and voltage characteristics and MPP depends on solar irradiations and ambient temperature. So a maximum power tracking control should be made rapidly in different temperature and solar radiation conditions. In this study; solar cell was obtained by using equivalent circuit of solar cell with Matlab / Simulink connected with dc-dc converter to fed brushless dc motor BLDC and water pumping system, this paper drive using adaptive neuro-fuzzy inference system (ANFIS) technique. The proposed (ANFIS) controller is trained off-line to identify the optimum output power of P-V system and desired water flow rate. This paper describes the operation of the system and the development of component models for the array, using ANFIS technique to enhance performance of system and to get the maximum power from P-V under different conditions of the solar insolation and temperature to get maximum flow rate of water to water pumping system WPS. An iteration technique which is mathematical-based is also presented for comparison and evaluation purposes. The paper indicates accuracy, robustness and effectiveness of the proposed models in water flow rate control, economic feasibility and fault detection.

Keywords: Maximum power Point tracking algorithms, Photovoltaics system & Adaptive Neuro-Fuzzy Inference System

1. Introduction

Solar renewable energy systems are more environmentally friendly than conventional energy sources over electricity generation. The advantages of using solar energy systems fall into two main categories: ecology and socioeconomic issues. From an ecological aspect, the use of solar energy technologies has various positive impacts that include reduction of greenhouse gas emissions (like CO₂, NO_x) and of toxic gas emissions (SO₂, particulates), prevention of soil pollution, reduction of transmission cost, and improvement in the quality of water resources [1–6]. The advantages of solar technologies comprise energy independency, employment opportunity creation [4, 5], acceleration of electrification of rural communities in isolated areas, and diversification and security (stability) of energy supply [2, 3, 7].

Photovoltaic (PV) systems sometimes called solar cells have found widespread application because they are simple, are compact, and have high power-to-weight ratio [8]. The PV system is the energy supply for many applications such as: water supply system in remote area where system is cost effective for long time duration which makes it suitable for grid-isolated rural locations. Without need for fuel or the extensive maintenance required by diesel pumps, Photo-Voltaic Water Pumping System (PVWPS) can provide clear water.

The output characteristic of PV cell depends mainly on the solar insolation and cell temperature. Variations in solar irradiance and cell operating temperature will nonlinearly affect the current voltage as well as power-voltage characteristics of a PV module [9]. In addition to the two parameters (i.e., solar irradiance and cell operating temperature), the performance of a PV module depends on its

- Higher speed ranges

operating point on I-V plane. Forcing a PV module to operate near Maximum power point (MPP) results in a higher efficiency. Hence, in order to extract maximum power output from a PV module it can be controlled by maximum power point tracking (MPPT) controller [11]. MPPT controllers track maximum possible power from the Photovoltaic panel [12]. Thus, use of MPPT controller is one way of optimizing the performance of PV module.

Researchers in [13-16] have been developed many studies in modeling, optimization and control about PVWPS, which are used to supply water for drinking and irrigation in remote regions. Gopal et al. [17], briefly review the recent published papers related to PVWPS and the importance of modeling using artificial intelligence.

Many researchers developed ANFIS models for prediction and water flow rate collected from PVWPS. In 2014 and 2015 [18-19]. In 2016 many papers [20-21] have been introduced review on modeling studies, and maximizing the discharge rate of PVWPS.

Brushless Direct Current (BLDC) motors are one of the motor types rapidly gaining popularity. BLDC motors are used in industries such as Appliances, Automotive, Aerospace, Consumer, Medical, Industrial Automation Equipment and Instrumentation. As the name implies, BLDC motors do not use brushes for commutation; instead, they are electronically commutated. BLDC motors have many advantages over brushed DC motors and induction motors. A few of these are:

- Better speed versus torque characteristics
- High dynamic response
- High efficiency
- Long operating life
- Noiseless operation

In addition, the ratio of torque delivered to the size of the motor is higher, making it useful in applications where space and weight are critical factors

2. Steady state model of PV system based on BLDC motor

2.1 modeling of the PV array

The energy of falling light impinging the PV cell is converted directly to DC energy. PV cells are connected in series and parallel combinations to form a PV module. In order to harvest more solar energy, PV modules are connected together to form PV arrays. Equivalent circuit of a PV array is shown in fig.2 Equations (2.1-2.4) present a general formula of a PV array modelling.

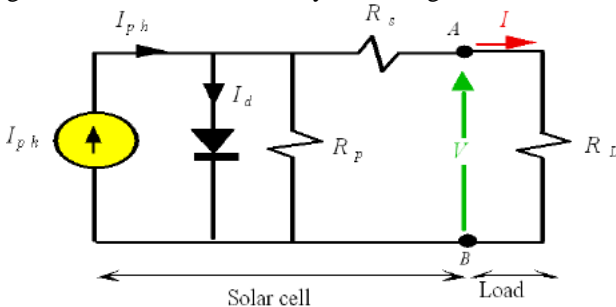


Fig.1 Equivalent circuit PV solar cell

$$I_{PV} = N_p [I_{ph} - I_{SA}] \quad (2.1.1)$$

$$I_{PV} = N_p [I_{ph} - I_{SA} \left[\exp \left(\frac{q \left(\frac{V_{PV}}{N_s} + I_{RS} \right)}{nkT} \right) - 1 \right] - \frac{N_p V_{PV} + N_s I_{PV} R_s}{N_s N_p R_{SH}}] \quad (2.1.2)$$

$$I_{ph} = \left(I_{sc} + K_i (T_c - T_{ref}) \right) * \frac{G}{G_{ref}} \quad (2.1.3)$$

$$I_{SA} = I_{rs} \left(\frac{T_c}{T_{ref}} \right)^3 \exp \left(\frac{q E_G}{K n} \left(\frac{1}{T_{ref}} - \frac{1}{T_c} \right) \right) \quad (2.1.4)$$

Where:

- I_{rs} : Reference saturation current,
- T_{ref} : Reference temperature (273 Kelvin),
- q: Electron charge ($1.6 \times 10^{-19} C$),
- G_{ref} : Reference irradiance ($1000 W/m^2$),
- I_{rs} : Array short circuit current at $25^\circ C$,
- K: Boltzmann constant ($1.38 \times 10^{-23} J/K$),
- V_{PV} : Array output voltage,
- R_{SH} : shunt module resistance,
- I_{PV} : Array output current,
- n: Diode ideality factor,
- I_{SA} : Array saturation current,
- K_i : Temperature coefficient,
- I_{ph} : Array photo current,

- T_c : module temperature (kelvin),
- I_{sh} : Array shunt current,
- N_p : number of parallel modules,
- N_s : number of series modules,
- R_s : series modules resistance,
- G: Solar irradiance ($1000 W/m^2$),
- E_G : band gap energy.

From equations (2.1-2.4), output power of PV modules depends mainly on solar insolation and operation temperature. The I-V and P-V characteristics at various temperatures shown in fig.2, and for various irradiance shown in fig.3

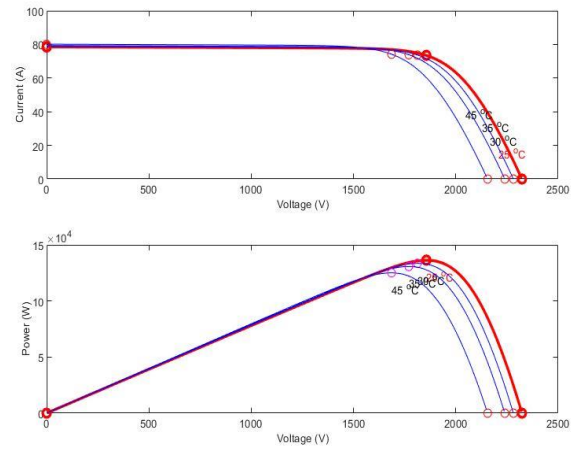


Fig.2 I-V and P-V characteristics at various temperature

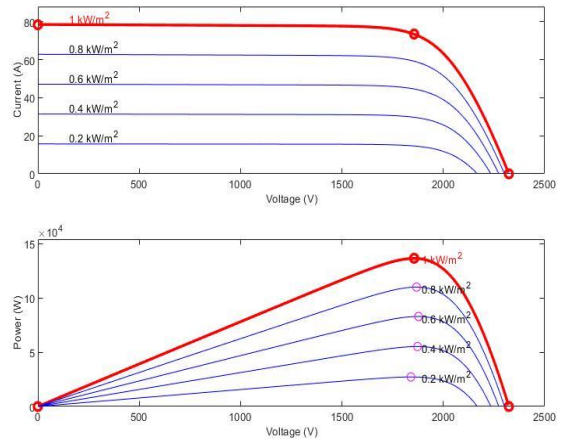


Fig.3 I-V and P-V characteristics at various irradiance

2.2 Modeling of Boost converter

A boost converter is one of the simplest types of switch mode converter. As the name suggests, it takes an input voltage and boosts or increases it. It is incorporated to step-up the PV array voltage to the dc-bus voltage level, along with tracking the MPP regardless the variation of environmental conditions. It contains two semiconductor power switches [IGBT (SW) & diode (D_{boost})] and one storage element (L),

as depicted in Fig. 4. The relation between the input and output voltage of the boost converter in steady state is indicated in eqn (2.2.1).

$$V_{out} = \frac{V_{in}}{(1-D)} \quad (2.2.1)$$

Where, V_{out} is the output voltage, and D is the duty cycle

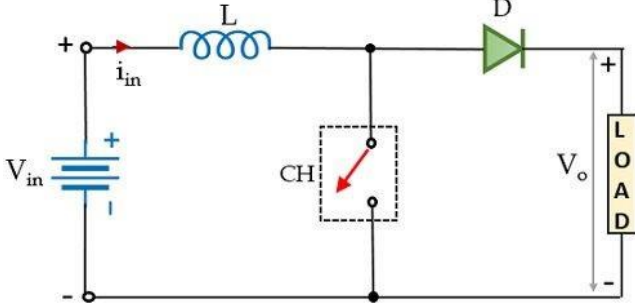


Fig.4. circuit of boost converter.

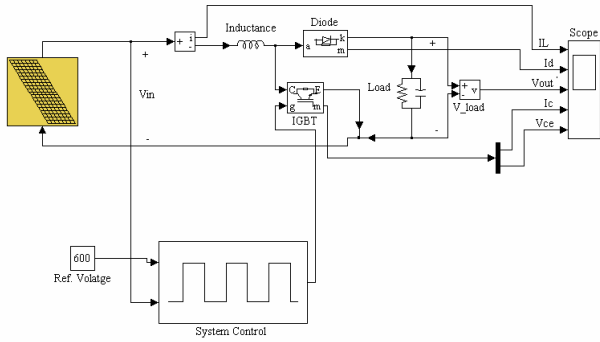


Fig. 5 Simulink Model for the Boost Converter.

2.3 Modeling of BLDC motor

In this paper a 3 phases, 4 poles, Y connected trapezoidal back-EMF type BLDC is modeled. Trapezoidal back-EMF is referring that mutual inductance between stator and rotor has trapezoidal shape [3]. Therefore abc phase variable model is more applicable than d-q axis. With the intention of simplifying equations and overall model the following assumptions are made:

- Magnetic circuit saturation is ignored.
- Stator resistance, self and mutual inductance of all phases are equal and constant.
- Hysteresis and eddy current losses are eliminated.
- All semiconductor switches are ideal.

The electrical and mechanical mathematical equations of BLDC are:

$$V_a = R_{ia} + (L - M) \frac{di_a}{dt} + E_a \quad (2.3.1)$$

$$V_b = R_{ib} + (L - M) \frac{di_b}{dt} + E_b \quad (2.3.2)$$

$$V_c = R_{ic} + (L - M) \frac{di_c}{dt} + E_c \quad (2.3.3)$$

$$\begin{aligned} E_a &= K_e \omega_m F(\theta_e) \\ E_b &= K_e \omega_m F(\theta_e - \frac{2\pi}{3}) \\ E_c &= K_e \omega_m F(\theta_e + \frac{2\pi}{3}) \end{aligned} \quad (2.3.4)$$

$$T_a = K_t i_a F(\theta_e)$$

$$T_b = K_t i_b F(\theta_e - \frac{2\pi}{3}) \quad (2.3.5)$$

$$T_c = K_t i_c F(\theta_e + \frac{2\pi}{3})$$

$$T_e = T_a + T_b + T_c \quad (2.3.6)$$

$$T_e - T_l = J \frac{d^2\theta}{dt^2} + \beta \frac{d\theta_m}{dt} \quad (2.3.7)$$

$$\theta_e = \frac{p}{2} \theta_m \quad (2.3.8)$$

$$\omega_m = \frac{d\theta_m}{dt} \quad (2.3.9)$$

Where $k = a, b, c$

V_k : K_{th} Phase voltage applied from inverter to BLDC,

I_k : k_{th} Phase current

R : Resistance of each phase of BLDC

M : Mutual inductance

L : Inductance of each phase of BLDC

E_k : k_{th} Phase back EMF

T_k : Electric torque produced by k_{th} phase

K_e : Back - EMF constant

T_e : Electric torque produced by BLDC

K_t : Torque constant

ω_m : Angular speed of rotor

θ_m : Mechanical angel of rotor

$F\theta_e$: Back - EMF reference as function of rotor position

θ_e : Electrical angel of rotor

BLDC coupled to a centrifugal pump to feed and control desired water flow rate, the pump power and torque equations under steady state are:

$$P_L = 9.810 * Q * H \quad (2.3.10)$$

$$T_L = K_p * W_m^2 \quad (2.3.11)$$

At steady state ($T_e = T_l$), load curve equation will be as follow :

$$K_p V_a^2 - 2K_p V_a I_a R_a - C_e^3 * I_a + K_p I_a^2 R_a^2 = 0 \quad (2.3.12)$$

According to operating point of the motor- pump system, the water flow rate can be calculated by equation:

$$9.810 * Q * H * C_e^3 = \eta_p K_p (V_a - I_a R_a)^2 \quad (2.3.13)$$

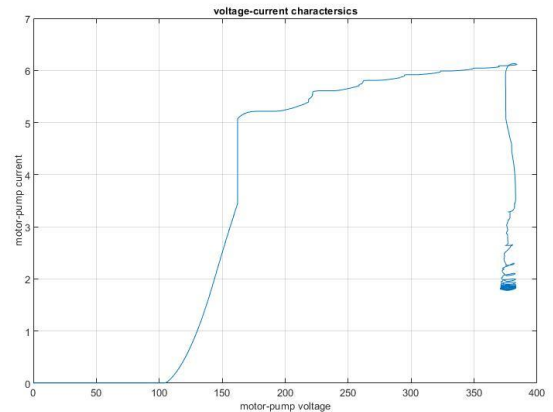


Fig.6. voltage-current characteristic

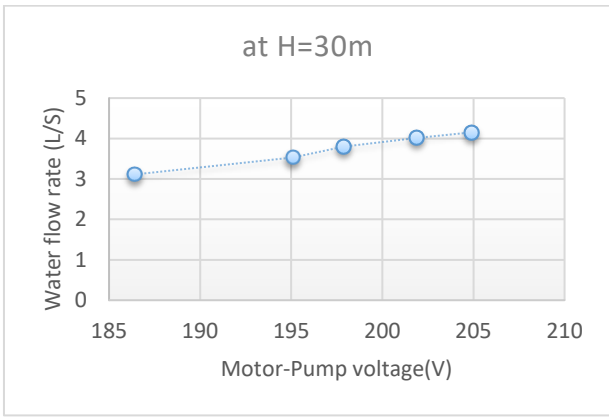


Fig.7.a Flow rate-voltage characteristic at H=30m

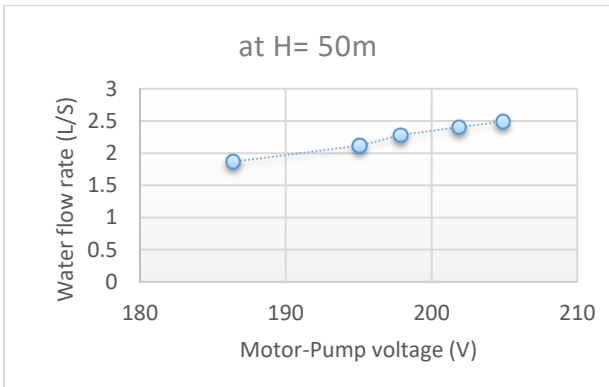


Fig.7.b Flow rate -voltage characteristic at H=50m

3. Operation of complete system

A complete system as shown in block diagram mainly consist of the PV array, boost converter, BLDC motor with integrated MPPT control, and centrifugal pump.

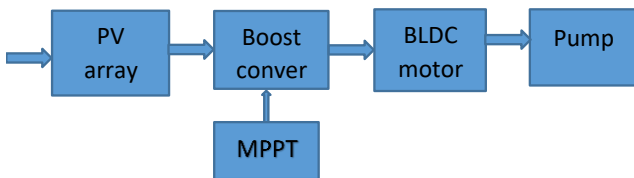


Fig.8. Block diagram of complete system

3.1. Performance analysis of complete system using iteration technique

Based on the preceding equations (2.1.1), (2.3.12) & (2.3.13) the operation of complete system was simulated using iteration technique , solar insolation (G), cell working temperature (T) and total static heads (H) effect on water flow rate (Q) , we can investigate this effect using iteration technique as shown in flow chart

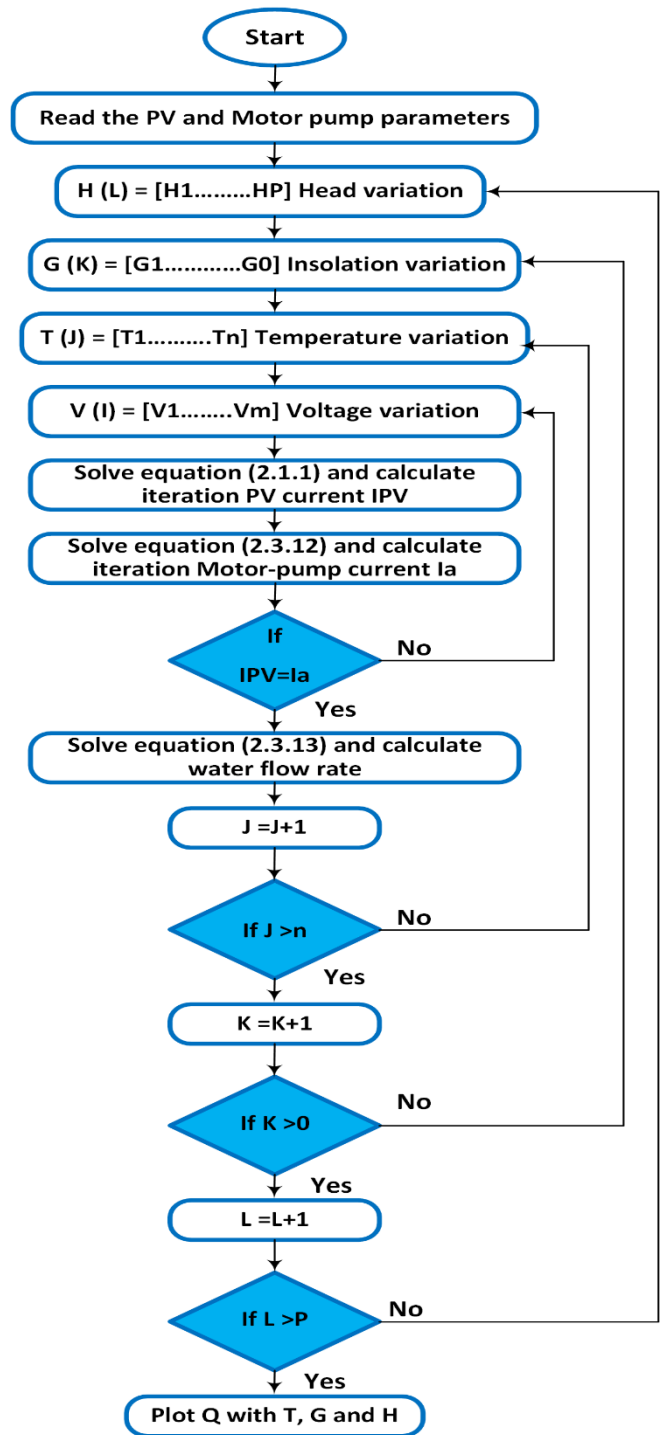


Fig.9. performance analysis of system using iteration technique

The water flow rate is calculated at different operating circumstances of various solar insolation (G), cell working temperature (T) variation and total static heads (H). So complete analysis is done at different loading as shown in fig.8, fig.9 & fig.10.

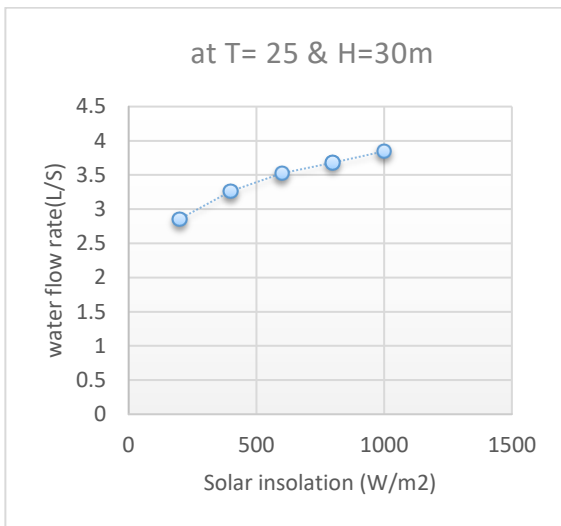


Fig.10. water flow rate at various solar insolation (G)

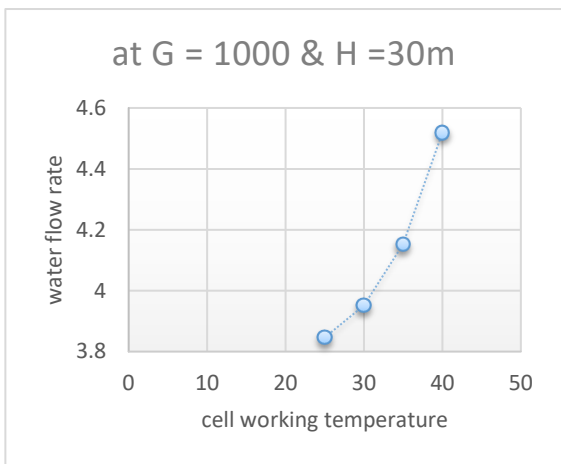


Fig.11. water flow rate at various cell working temperature (T)

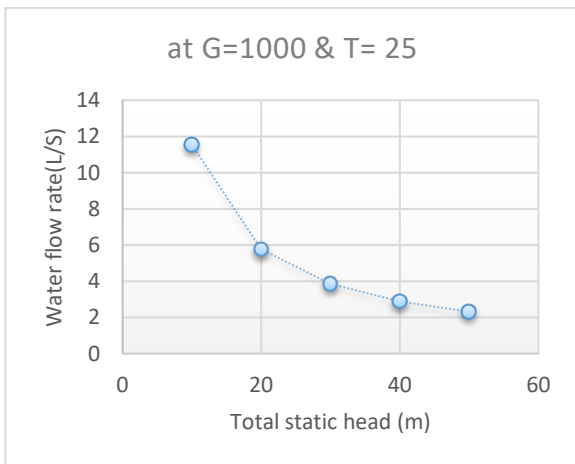


Fig.12. water flow rate at various total static head (H)

3.2 performance analysis using Adaptive Neuro-Fuzzy Inference System (ANFIS)

ANFIS is a simple data learning technique that uses Fuzzy Logic to transform given inputs into a desired Output. This transformation is achieved through highly interconnected Neural Network processing elements and information

pattern	Inputs				Q (L/sec)	Q (L/sec)
	T	G	D	H	Iteration technique	ANFIS technique
1	25	1000	0	30	3.8464	3.8466
2	25	800	0	30	3.6799	3.6778
3	25	600	0	30	3.5270	3.5298
4	25	400	0	30	3.2630	3.2609
5	25	200	0	30	2.8569	2.8576
6	25	200	0.05	30	3.3310	3.3317
7	25	200	0.1	30	4.2134	4.2127
8	35	1000	0	30	4.1522	4.156
9	35	800	0	30	4.0129	3.9944
10	35	600	0	30	3.7988	3.824
11	35	400	0	30	3.5304	3.5229
12	35	200	0	30	3.1108	3.1075
13	35	200	0	20	4.6662	3.6801
14	35	400	0	20	5.2956	5.2676
15	35	600	0	20	5.6983	5.7239
16	35	800	0	20	6.0194	5.9996
17	35	1000	0	20	6.2283	6.2366
18	35	1000	0	50	2.4913	2.4894
19	35	800	0	50	2.4077	2.4149
20	35	600	0	50	2.2793	2.2696
21	35	600	0.05	50	2.6504	2.6512
22	35	600	0.1	50	3.3089	3.3081
23	35	400	0	50	2.1182	2.1392
24	35	400	0.05	50	2.4750	2.4759
25	35	400	0.1	50	3.0928	3.0925
26	35	400	0.15	50	4.0673	4.0502

connections, which are weighted to map the numerical inputs into an output. ANFIS combines into a single technique, having the benefits of the two machine learning techniques, providing adaptability due to the neural network (NN) Back propagation and smoothness, due to the fuzzy controller (FC) interpolation [22]. ANFIS works by applying Neural Network learning methods to tune the parameters of a Fuzzy Inference System (FIS). ANFIS has a five-layer architecture [23].

In this work, the ANFIS model is based upon a first order Takagi-Sugeno model. Fig. 11 shows the five layers ANFIS network which have been used, with Gaussian2 membership function where it is given a good outputs compared the others membership functions.

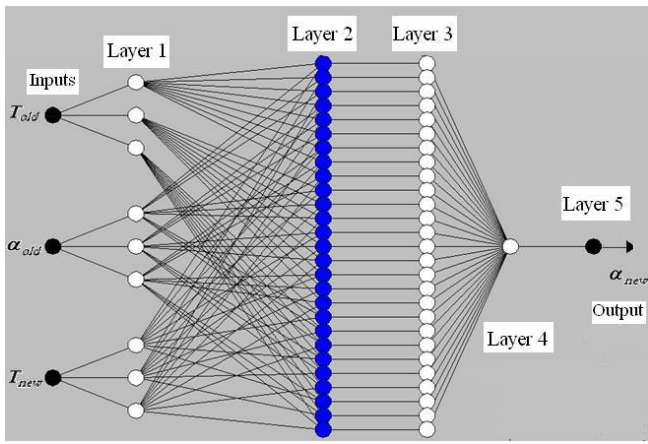


Fig. 11. Construction of the adopted Adaptive Neuro-Fuzzy Inference System model

Table 1. Shows sample of data using for testing performance of the system at different operation conditions using iteration technique and ANFIS technique.

The Mean Sum Square Error (MSSE) at different iteration data can be obtained as follow:

$$MSSE = \frac{\sum_1^{paeerens} (Q_{iteration} - Q_{ANFIS})^2}{number\ of\ patterns} \quad (3.2.1)$$

MSSE for ANFIS technique is $1.884615 \cdot 10^{-8}$

4. Conclusion

Water flow rate of the system using conventional iteration technique has been found to be complex and take long time with mathematical procedures. The application of ANFIS technique has been demonstrated and has been found to be very effective.

REFERENCES

[1] A. Abu-Zour and S. Riffat, "Environmental and economic impact of a new type of solar louvre thermal collector," *International Journal of Low-Carbon Technologies*, vol. 1, no. 3, pp. 217–227, 2006.

[2] W. Charters, "Developing markets for renewable energy technologies," *Journal of Renewable Energy*, vol. 22, no. 1-3, pp. 217–222, 2001.

[3] K. Jagoda, R. Lonseth, A. Lonseth, and T. Jackman, "Development and commercialization of renewable energy technologies in Canada: An innovation system perspective," *Journal of Renewable Energy*, vol. 36, no. 4, pp. 1266–1271, 2011.

[4] J. M. Cansino, M. D. P. Pablo-Romero, R. Roman, and R. Yñiguez, "Tax incentives to promote green electricity: an overview of EU-27 countries," *Energy Policy*, vol. 38, no. 10, pp. 6000–6008, 2010.

[5] R. E.H. Sims, H.-H. Rogner, and K. Gregory, "Carbon emission and mitigation cost comparisons between fossil fuel, nuclear and renewable energy resources for electricity generation," *Energy Policy*, vol. 31, no. 13, pp. 1315–1326, 2003.

[6] T. J. Dijkman and R.M. J. Benders, "Comparison of renewable fuels based on their land use using energy densities," *Renewable & Sustainable Energy Reviews*, vol. 14, no. 9, pp. X3148–3155, 2010.

[7] P. D. Lund, "Effects of energy policies on industry expansion in renewable energy," *Journal of Renewable Energy*, vol. 34, no. 1, pp. 53–64, 2009.

[8] M. A. Eltawil and D. V. K. Samuel, "Vapor compression cooling system powered by solar PV array for potato storage," *Agricultural Engineering International: e CIGR E-Journal Manuscript*, vol. IX, 2007.

[9] Z. Salameh, *Renewable Energy System Design*, Elsevier Academic Press, 1st edition, 2014.

[11] S. S. Chandel, M. Nagaraju Naik, and R. Chandel, "Review of solar photovoltaic water pumping system technology for irrigation and community drinking water supplies," *Renewable & Sustainable Energy Reviews*, vol. 49, articleno.4338, pp. 1084–1099, 2015.

[12] G. Li, Y. Jin, M. Akram, and X. Chen, "Research and current status of the solar photovoltaic water pumping system – A review," *Renewable & Sustainable Energy Reviews*, vol. 79, pp.440–458, 2017.

[13] B.G. Belgacem, "Performance of submersible PV water pumping systems in Tunisia", *Energy for Sustainable Development*, Vol. 16, pp. 415–420, 2012.

[14] A. Boutelhig, Y. Bakelli, I. Hadj Mahammed, and, A. Hadj Arab, "Performances study of different PV powered DC pump configurations for an optimum energy rating at different heads under the outdoor conditions of a desert area", *Energy*, Vol. 39, pp. 33-39, 2012.

[15] A.E. Badoud, M. Khemliche, B. OuldBouamama, S. Bacha, Lavado, snd, L.F. Villa, "Bond graph modelling and optimization of photovoltaic pumping system: Simulation and experimental results ", *Simulation Modelling Practice and Theory*, Vol. 36, pp. 84–103, 2013.

[16] S. Haddad, A. Mellit, M. Benghanem, and, K.O. Dafallah, "Modelling and Estimation of the Hourly Flow Rate of a Photovoltaic Water Pumping System Using Polynomial Regression Method: Experimental Validation ", *International Scientific Journal Environmental Science*, Vol. 3, Issue 2 , pp 93- 97, June 2014.

[17] C. Gopal, M. Mohanraj, P. Chandramohan, and, P. Chandrasekar, " Renewable energy source water pumping systems —A literature review," *Renewable and Sustainable Energy Reviews*, Vol. 25, pp. 351–370, 2013.

[18] S. Haddad, A. Mellit, M. Benghanem, and, K.O. Dafallah, " ANNs-based modelling and prediction of hourly flow rate of a photovoltaic water pumping system: Experimental validation ", *Renewable and Sustainable Energy Reviews*, Vol. 43, pp. 635–643, March 2015.

[19] R. K. Kharb, S. L. Shimi, S. Chatterji, and, M. F. Ansari, "Modelling of solar PV module and maximum power point tracking using ANFIS ", *Renewable and Sustainable Energy Reviews*, Vol. 33, pp. 602–612, March 2014.

[20] Menghal, P.M. and Laxmi, A.Jaya, " Adaptive Neuro Fuzzy based dynamic simulation of induction motor drives' IEEE International Conference on Fuzzy Systems (FUZZ), 2013, Hyderabad, India

[21] A. Chermitti, O. Boukli-Hacene, A. Meghebbar, N. Bibitriki, and A. Kherous, "Design of a library of components for autonomous photovoltaic system under MATLAB/Simulink", *Physics Procedia*, Vol. 55, pp. 199 - 206, 2014.

[22] Simon, R. and Geeth a, A., " Comparison on the performance of Induction motor control using fuzzy and ANFIS controllers", *IEEE International Conference on Emerging Trends in Computing, Communication and Nano technology (ICE-CCN)*, 2013, Tirunelveli, India.

[23] J.S.R. Jang, "ANFIS: Adaptive-Network-Based Fuzzy Inference System ", *IEEE Trans. Systems, Man, and Cybernetics*, vol. 23, no. 3, pp. 665-684, May/June 1993.